Electronic Supplementary Information

A non-fused mono-*meso*-free pentaphyrin and its rhodium(I) complex

Tomoki Yoneda, [a] **Hirotaka Mori,** [a] **Byung Sun Lee,** [b] **Min-Chul Yoon,** [b]
Dongho Kim*[b] **and Atsuhiro Osuka***[a]

[a]*Department of Chemistry, Graduate School of Science, Kyoto University,*
Sakyo-ku, Kyoto 606-8502, Japan
[b] *Spectroscopy Laboratory for Functional π-electronic Systems and Department of chemistry, Yonsei University, Seoul 120-749, Korea.*

Contents

1. General Information

All reagents were of the commercial reagent and were used without further purification except where noted. The spectroscopic grade dichloromethane was used as solvent for all spectroscopic studies. Silica gel column chromatography was performed on Wakogel C-300 or C-400. Thin-layer chromatography (TLC) was carried out on aluminum sheets coated with silica-gel 60 F_{254} (Merck 5554)

UV/visible spectra were recorded on a Shimazu UV-3100PC spectrometer. ^{1}H, ^{13}C and ^{19}F NMR spectra were recorded on a JEOL ECA-600 spectrometer (operating as 600.17 MHz for ^{1}H, 564.73 MHz for ^{19}F) using the residual solvent as the internal reference for ^{1}H (δ = 7.26 ppm in $CDCl_3$), hexafluorobenzene for ^{19}F (δ = –162.9 ppm) was employed as external references. High-resolution electrospray-ionisation time-of-flight mass spectroscopy (HR-ESI-TOF-MS) was recorded on a BRUKER microTOF model using negative or positive mode for acetonitrile solutions of samples.

Two-photon absorption experiments

The two-photon absorption (TPA) spectrum was measured in the NIR region using the open-aperture Z-scan method with 130 fs pulses from an optical parametric amplifier (Light Conversion, TOPAS) operating at a repetition rate of 3 kHz generated from a Ti:sapphire regenerative amplifier system (Spectra-Physics, Hurricane). After passing through a 10 cm focal length lens, the laser beam was focused and passed through a 1 mm quartz cell. Since the position of the sample cell could be controlled along the laser beam direction (*z* axis) using the motorcontrolled delay stage, the local power density within the sample cell could be simply controlled under constant laser intensity. The transmitted laser beam from the sample cell was then detected by the same photodiode as used for reference monitoring. The on-axis peak intensity of the incident pulses at the focal point, I_0, ranged from 40 to 60 GW cm^{-2}. For a Gaussian beam profile, the nonlinear absorption coefficient can be obtained by curve fitting of the observed open-aperture traces $T(z)$ with the following equation:

$$T(z)=1-\frac{\beta I_0(1-e^{-\alpha_0 l})}{2\alpha_0[1+(z/z_0)^2]}$$

where α_0 is the linear absorption coefficient, l the sample length, and z_0 the diffraction length of the incident beam. After the nonlinear absorption coefficient has been obtained, the TPA cross section $\sigma^{(2)}$ of one solute molecule (in units of GM, where 1

GM = 10^{-50}cm^4 s photon^{-1} molecule^{-1}) can be determined by using the following relationship:

$$\beta = \frac{10^{-3}\sigma^{(2)}N_A d}{h\nu}$$

where N_A is the Avogadro constant, d is the concentration of the compound in solution, h is the Planck constant, and v is the frequency of the incident laser beam.

Transient absoption experiments

The femtosecond time-resolved transient absorption (TA) spectrometer used for this study consisted of a femtosecond optical parametric amplifier (Quantronix, Palitra-FS) pumped by a Ti:sapphire regenerative amplifier system (Quantronix, Integra-C) operating at 1 kHz repetition rate and an accompanying optical detection system. The generated OPA pulses had a pulse width of ~100 fs and an average power of 1 mW in the range 450 to 800 nm, which were used as pump pulses. White light continuum (WLC) probe pulses were generated using a sapphire window (2 mm thick) by focusing of small portion of the fundamental 800 nm pulses, which were picked off by a quartz plate before entering into the OPA. The time delay between pump and probe beams was carefully controlled by making the pump beam travel along a variable optical delay (Newport, ILS250). Intensities of the spectrally dispersed WLC probe pulses were monitored by miniature spectrograph (OceanOptics, USB2000+). To obtain the time-resolved transient absorption difference signal (ΔA) at a specific time, the pump pulses were chopped at 25 Hz and absorption spectra intensities were saved alternately with or without pump pulse. Typically, 6000 pulses were used excite samples and to obtain the TA spectra at a particular delay time. The polarisation angle between pump and probe beam was set at the magic angle (54.7° using a Glan-laser polarizer with a half-wave retarder to prevent polarisation-dependent signals. The cross-correlation fwhm in the pump-probe experiments was less than 200 fs, and chirp of WLC probe pulses was measured to be 800 fs in the 400-800 nm regions. To minimize chirp, all reflection optics were used in the probe beam path, and a quartz cell of 2 mm path length was employed. After completing each set of fluorescence and TA experiments, the absorption spectra of all compounds were carefully checked to rule out the presence of artifacts or spurious signals arising from, for example, degradation or photo-oxidation of the samples in question.

2. Synthesis and characterisation

meso-free 1,9-bis(pentafluorobenzoyl)dipyrromethane 9

A solution of dipyrromethane (1.0 g, 6.8 mmol) in dry toluene (50 mL) was treated with a solution of MesMgBr in THF (1.0 M, 20.5 mmol; 3.0 equiv) at 0 °C. After 15 min, pentafluorobenzoyl chloride (2.0 mL, 13.7 mmol; 2.0 equiv) was added slowly to the reaction mixture and the resultant solution was stirred for an additional 15 min. Then, the slow addition of MesMgBr (1.0 M, 20.5 mmol; 3.0 equiv) and the aroyl chloride (2.0 mL, 13.7 mmol; 2.0 equiv) was repeated during 30 min. After being stirred for 60 min at ambient temperature, the reaction mixture was quenched by addition of a saturated aqueous NH_4Cl solution (100 mL). Product was extracted with ethyl acetate. The combined organic extract was washed with water and dried over anhydrous Na_2SO_4. After the solvent was removed, precipitation from CH_2Cl_2/hexane afforded crude product, which was purified by recrystallization from cooled CH_2Cl_2/hexane to give white powder of **9** (2.44 g; 67%).

^{1}H NMR (600 MHz, $CDCl_3$) δ [ppm] = 10.60 (s, 2H; NH), 6.69 (d, J = 6.2 Hz, 2H, β), 6.23 (d, J = 6.2 Hz, 2H, β), 4.17 (s, 2H, *meso*-H); ^{19}F NMR (565 MHz, $CDCl_3$) δ [ppm] = –139.90 (d, J = 20.7 Hz, 2F; *o*-F), –150.72 (t, J = 20.7 Hz, 1F; *p*-F), and –163.19 (m, 2F, *m*-F) HR-ESI TOF-MS m/z = 533.0353 (calcd for $C_{23}H_8N_2O_2F_{10}$ = 533.0353 $[M{-}H]^-$)

5,10,15,20-tetrakis(pentafluorophenyl) mono-*meso*-free [22]pentaphyrin(1.1.1.1.1) 7

meso-free 1,9-bis(pentafluorobenzoyl)dipyrromethane **9** (266 mg, 0.50 mmol) was reduced with $NaBH_4$ (380 mg, 10 mmol) in a 10:1 mixture solution of THF and methanol (110 mL). After 1 h, the reaction was quenched with water and the products were extracted with ethyl acetate. The organic phase was washed with brine and dried over anhydrous Na_2SO_4. The solvent was removed under reduced pressure to yield di-carbinol quantitatively, which was unstable at ambient temperature and hence had to be used immediately. The di-carbinol was added to a solution of 5,10-bis(pentafluorophenyl)tripyrrane (279 mg, 0.5 mmol) in dry CH_2Cl_2 (100 mL). After the resultant solution was stirred under N_2 atmosphere for 5 min, *p*-toluenesulfonic acid monohydrate (9.5 mg, 0.1 eq) was added and stirring was continued for 30 min. DDQ (558 mg, 2.5 mmol) was added and the resulting solution was stirred for further 30 min. The reaction mixture with 100 mL of ethyl acetate was passed through a basic alumina column with followed by evaporation of solvent under reduced pressure. The residue was purified by silica gel chromatography using CH_2Cl_2. After evaporation of the red fraction to dryness yielded a crude product of *meso*-free pentaphyrin **7**. The UV/vis absorption spectrum was collected after further purification by gel permeation chromatography following silica-gel column chromatography. The fraction was directly used for the measuement.

^1H NMR (600MHz, $CDCl_3$): δ [ppm] = 9.66 (t, J = 4.1 Hz, 2H; β), 9.09 (s, 2H, β), 8.91 (s, 4H; β), 1.64 (s, 2H; NH), –1.82 (d, J = 2.8 Hz, 2H; β), –6.14 (s, 1H; *meso*-H) ^{19}F NMR (565 MHz, $CDCl_3$): δ [ppm] = –134.4 (s, 2F; *o*-F), –137.2 (d, J = 20.7 Hz, 2F; *o*-F), –138.0 (d, J = 20.7 Hz, 2F; *o*-F), –141.0 (d, J = 20.7 Hz, 2F; *o*-F), –150.6 (t, J = 20.7 Hz 2F; *p*-F), –151.2 (t, J = 20.7 Hz 2F; *p*-F), –160.2 (brs, 2F; *m*-F), –160.4 (brs, 2F; *m*-F), –162.0 (brs, 2F; *m*-F), –162.8 (brs, 2F; *m*-F), ESI-MS: *m/z*: 1050.0775 $[M–H]^-$; calcd for $C_{49}H_{13}N_5F_{20}$: 1050.0768; UV/vis (CH_2Cl_2): λ_{max} [nm] = 509, 645, 694, 754 and 831 nm.

5,10,15,20-tetrakis(pentafluorophenyl) mono-*meso*-free [22]pentaphyrin(1.1.1.1.1) bis-rhodium(I) complex 12

$[RhCl(CO)_2]_2$ (194 mg, 0.5 mmol) was added to a solution of the crude mixture of mono-*meso*-free pentaphyrin **7** (synthesised upon noted procedure) in dry CH_2Cl_2 (150 mL). The reaction solution was stirred in the presence of NaOAc (205 mg, 2.5 mmol) under Ar atmosphere at room temperature. After 20 h, the reaction mixture was passed through short silica-gel column with CH_2Cl_2. After evaporation of the solvent, the residue was subjected to separation by silica-gel column chromatography using CH_2Cl_2 as the eluent to give a pink fraction of **12** (69 mg, 10%).

^1H NMR (600 MHz, $CDCl_3$): δ [ppm] = 8.89 (d, J = 4.8 Hz, 2H; β), 8.53 (d, J = 4.4 Hz, 2H, β), 8.27 (dd, J = 4.8, 4.4 Hz, 2H; β (coupled with the 2-fluorine atom in the pentafluorophneyl groups at 5 and 20-position)), 7.98 (d, J = 4.8 Hz, 2H; β) –2.84 (s, 1H; *meso*-H), –5.11 (s, 2H; β), ^{19}F NMR (565 MHz, $CDCl_3$): δ [ppm] = –133.1 (s, 2F; *o*-F), –135.4 (d, J = 13.8 Hz, 2F; *o*-F), –138.2 (dd, J = 24.1, 7.0 Hz, 2F; *o*-F), –141.0 (d, J = 24.1, 6.9 Hz, 2F; *o*-F), –150.4 (t, J = 20.7 Hz 2F; *p*-F), –150.8 (t, J = 20.7 Hz, 2F; *p*-F), –160.6 (m, 4F; *m*-F), –161.8 (t, J = 20.7 Hz, 2F; *m*-F), –162.4 (m, 2F; *m*-F), , ESI-MS: *m/z*: 1367.8656 $[M–H]^-$; calcd for $C_{53}H_{11}N_5F_{20}O_4Rh_2$: 1367.8675; UV/vis ($CH_2Cl_2$): λ_{max} [nm] (ε $[M^{-1}cm^{-1}]$) 344(31000), 539(121000), 683(11000), 722(11000) and 794 (3800).

2. NMR Spectra

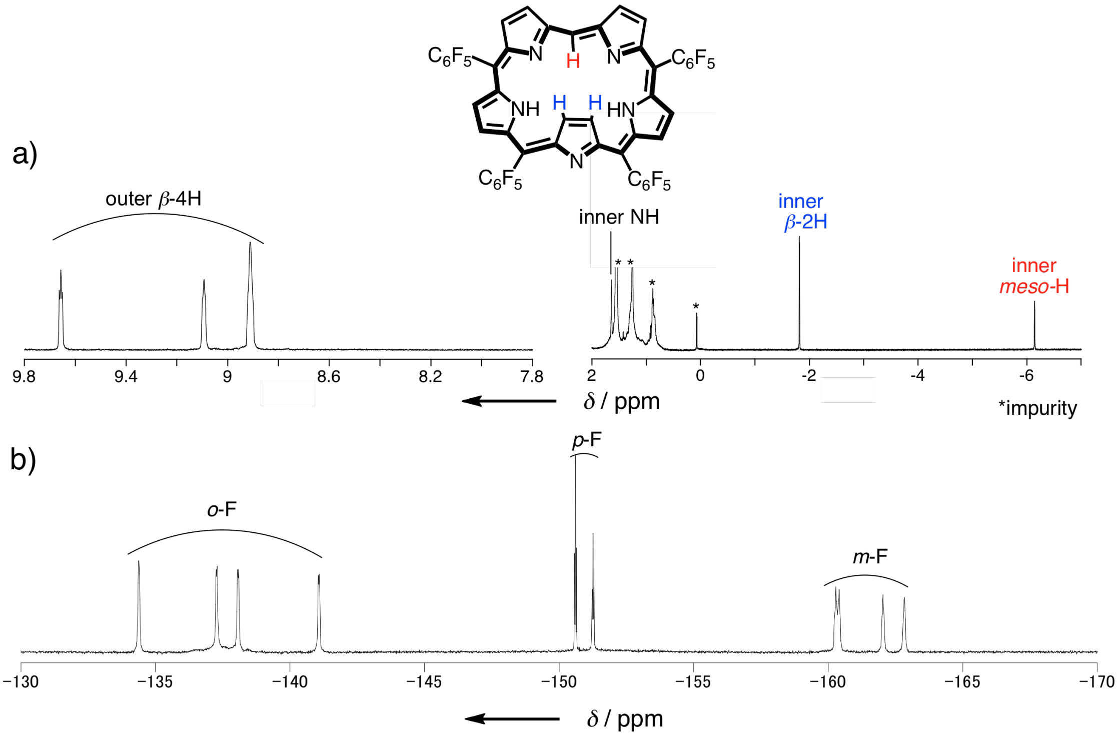

Fig. S1 a)^{1}H and b)^{19}F NMR spectra of **7** in $CDCl_3$ at 25 °C.

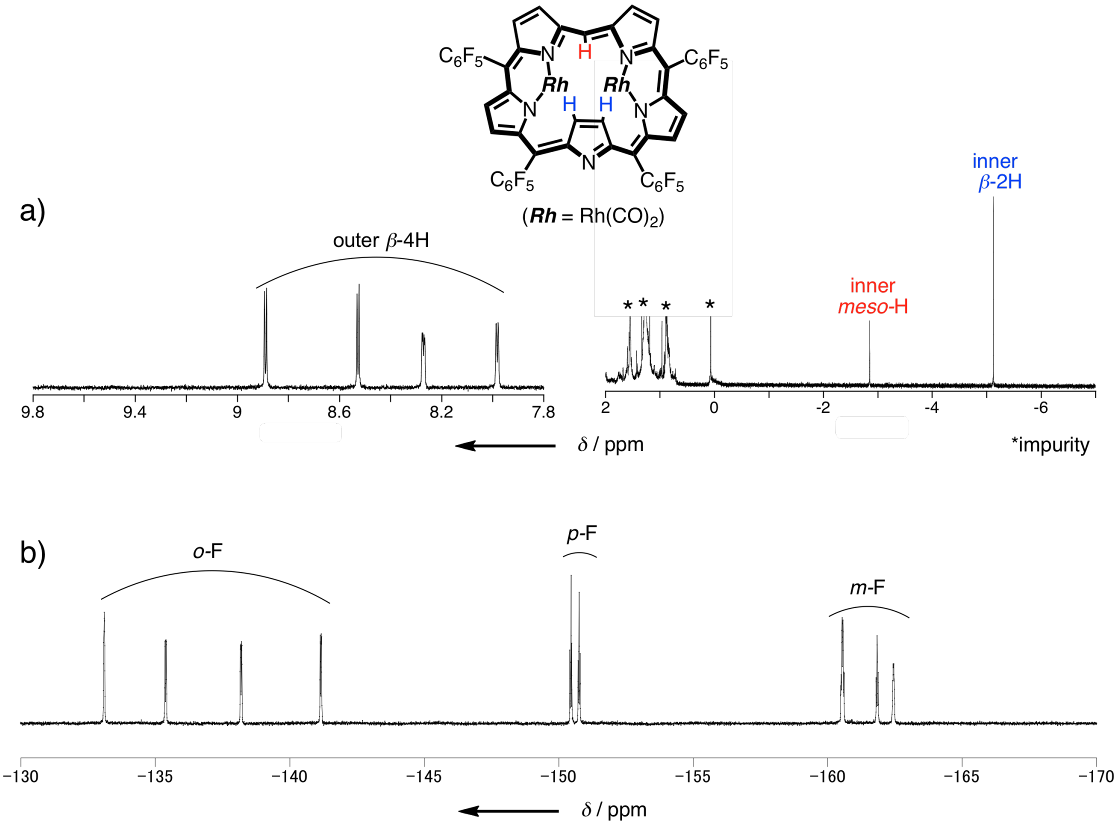

Fig. S2 a)^{1}H and b)^{19}F NMR spectra of **12** in $CDCl_3$ at 25 °C.

3. HR-ESI-TOF mass spectra

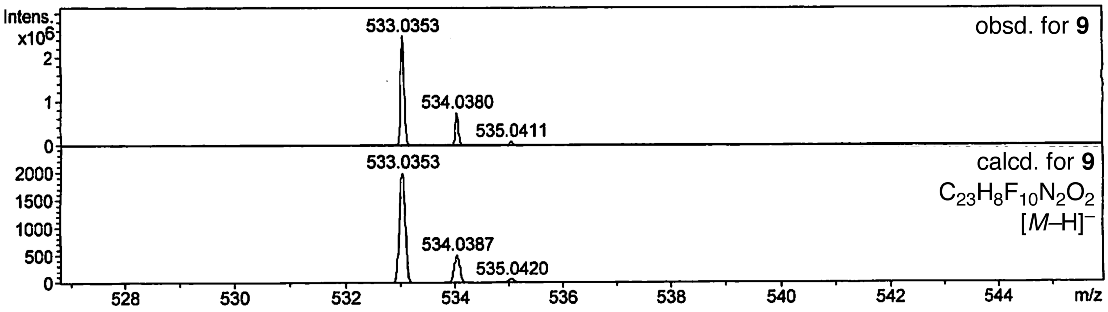

Fig. S3 HR-ESI-TOF mass spectra of **9** in CH_3CN.

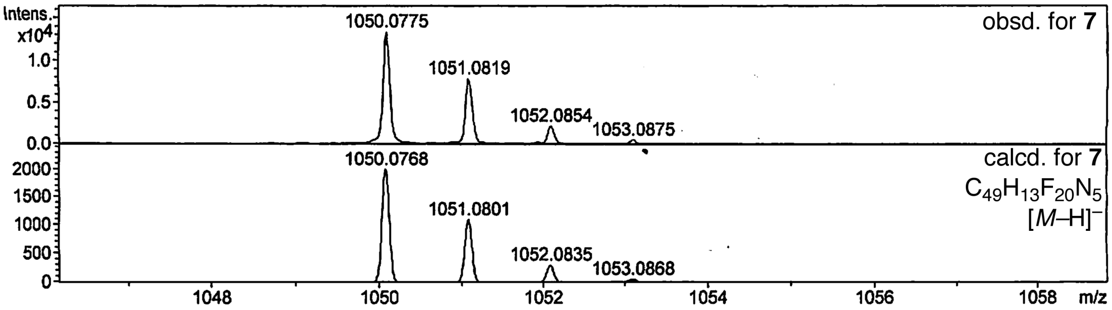

Fig. S4 HR-ESI-TOF mass spectra of **7** in CH_3CN.

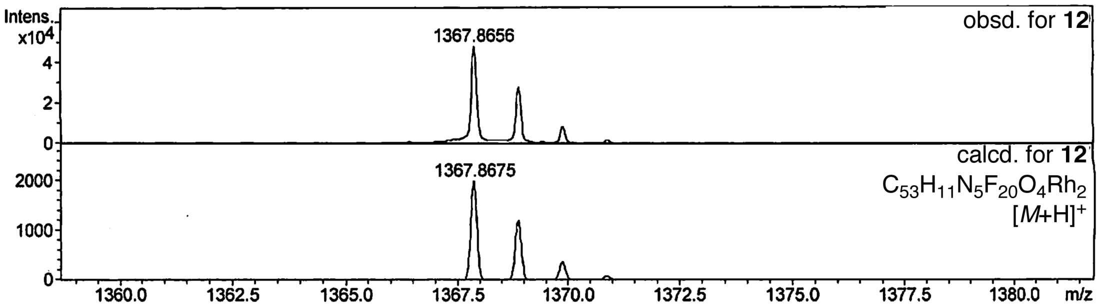

Fig. S5 HR-ESI-TOF mass spectra of **12** in CH_3CN.

4. X-ray diffraction analysis

Data for compound **12** was collected at –180 °C with a Rigaku RAXIS-RAPID diffraction by using graphite monochromated Cu-K_α radiation (λ = 1.54187 Å). The structures were solved by direct method (SHELXS-97).

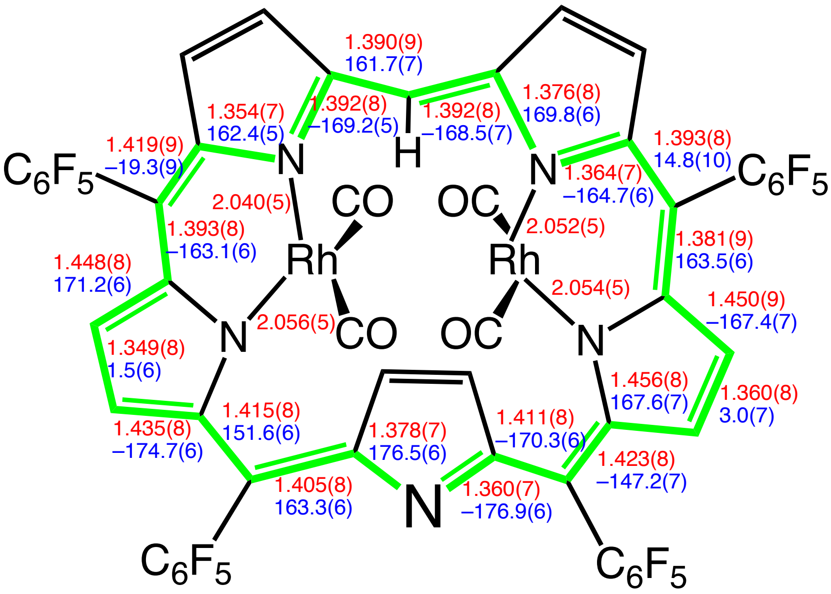

Fig. S6 Detailed structural data of **12**. The conjugated 22π-electron circuit (green), along which bond lengths in Å (numbers in red), and dihedral angles in deg (numbers in blue) are indicated.

5. Absorption spectra

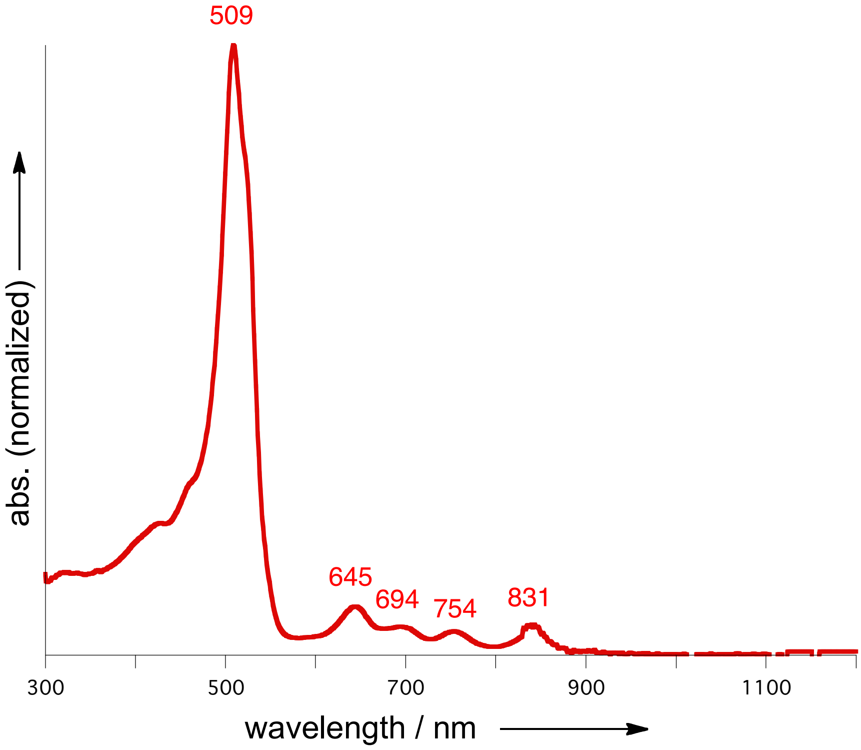

Fig. S7 UV/Vis absorption spectrum of **7** in CH_2Cl_2.

6. DFT calculation

DFT Calculations

All calculations were carried out using the *Gaussian 09* program.[15] All structures were fully optimized without any symmetry restriction. The calculations were performed by the density functional theory (DFT) method with restricted B3LYP (Becke's three-parameter hybrid exchange functionals and the Lee-Yang-Parr correlation functional) level, employing a basis set 6-31G(d) for C, H, N, O, F, and LANL2DZ for Rh. The NICS values and absolute ^{1}H shielding values were obtained with the GIAO method. The ^{1}H chemical shift values were calculated relative to $CHCl_3$ ($\delta = 7.26$ ppm, absolute shielding: 24.95 ppm). The global ring centres for the NICS values were designated at the nonweighted means of the carbon and nitrogen coordinates on the peripheral positions of conjugated macrocycles. In addition, NICS values were also calculated on centres of other local cyclic structures as depicted in the figures.

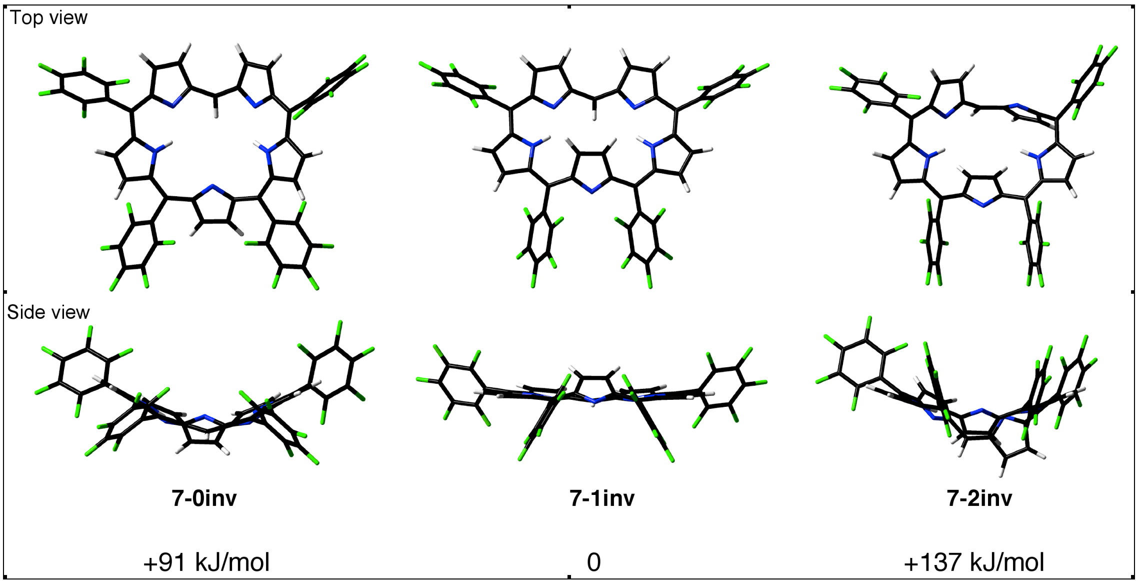

Fig. S8 Optimized structures and relative energies of conformers of 7.

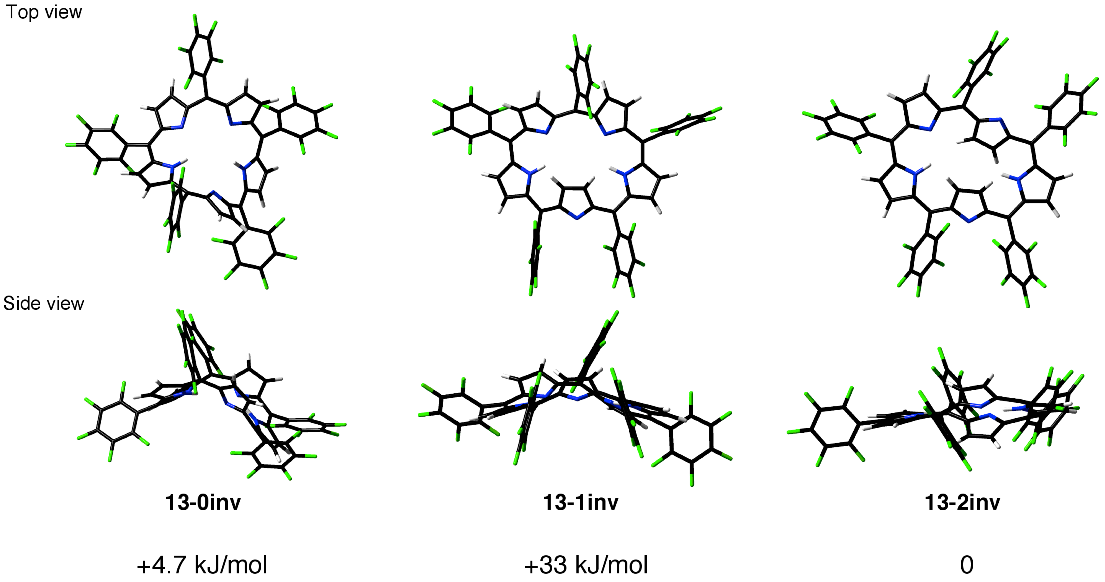

Fig. S9 Optimized structures and relative energies of conformers of non-fused *meso*-pentakis pentafluorophenyl substituted pentaphyrin **13**.

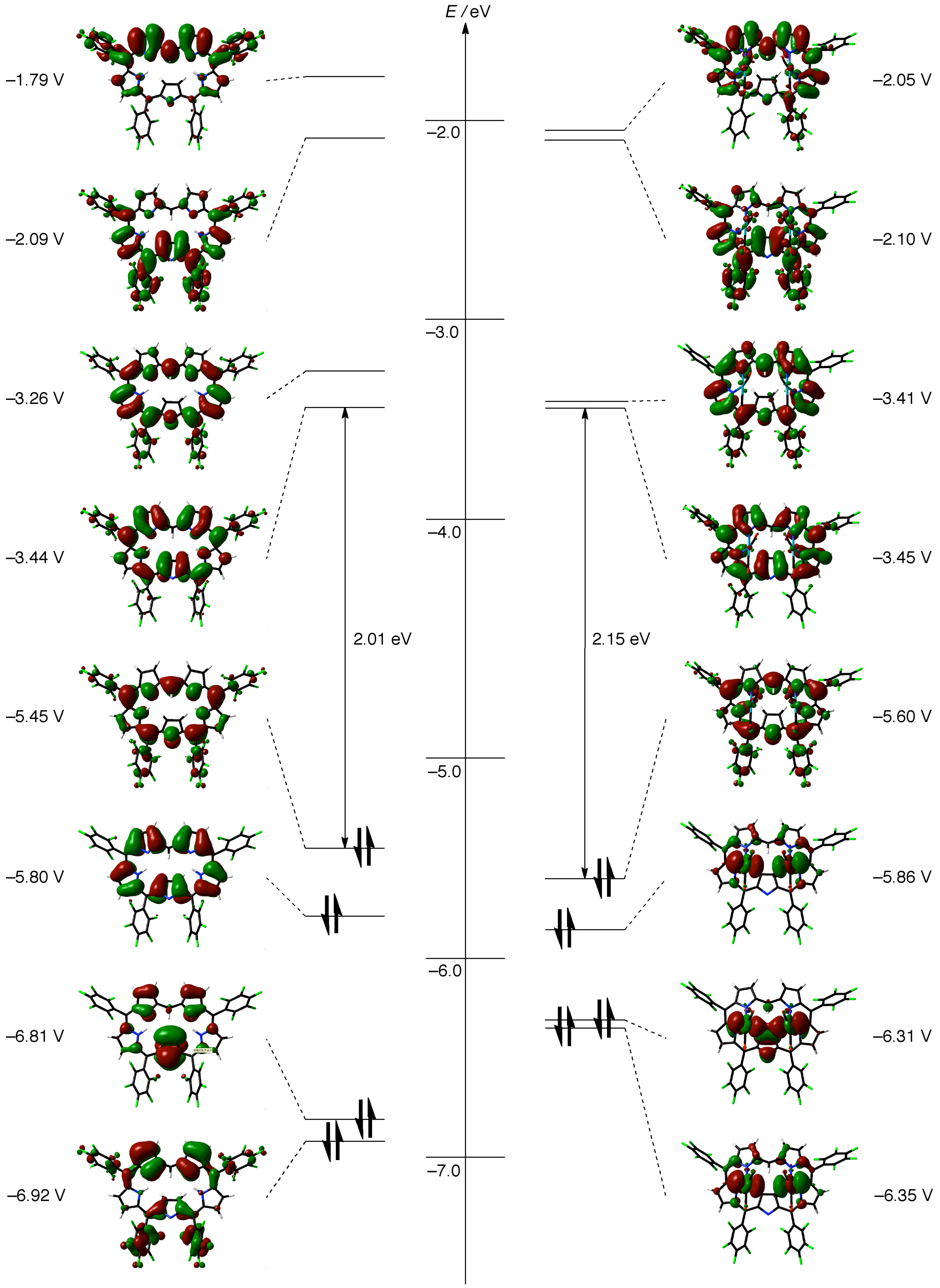

Fig. S10 Selected molecular orbitals of **7**(left) and **12**(right) on the optimized structures.

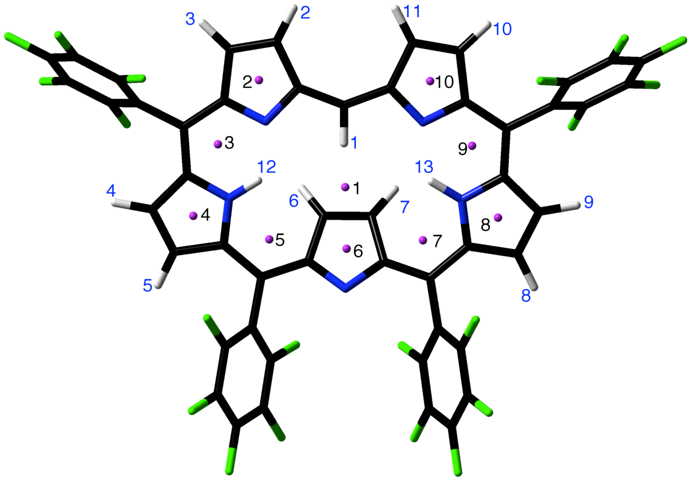

position	NICS (ppm)	^{1}H	δ (ppm)
1	–17.44	1	–8.17
2	0.11	2	9.36
3	–19.37	3	8.65
4	–10.93	4	9.05
5	–19.31	5	9.20
6	–13.18	6	–3.09
7	–19.31	7	–3.09
8	–10.93	8	9.20
9	–19.37	9	9.05
10	0.11	10	8.65
		11	9.36
		12	–3.36
		13	–3.36

Fig. S11 NICS values at various positions and simulated chemical shifts of **7** on the optimized structure.

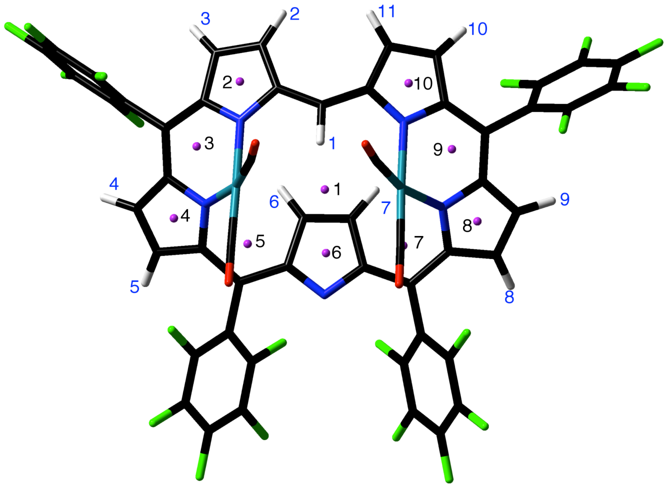

position	NICS (ppm)	^{1}H	δ (ppm)
1	–21.80	1	–4.94
2	–5.02	2	8.31
3	–18.27	3	7.34
4	–6.35	4	8.23
5	–19.40	5	8.41
6	–12.32	6	–5.95
7	–19.51	7	–6.04
8	–6.86	8	8.22
9	–18.09	9	7.71
10	–4.80	10	7.79
		11	8.42

Fig. S12 NICS values at various positions and simulated chemical shifts of **12** on the optimized structure.

7. TPA spectra

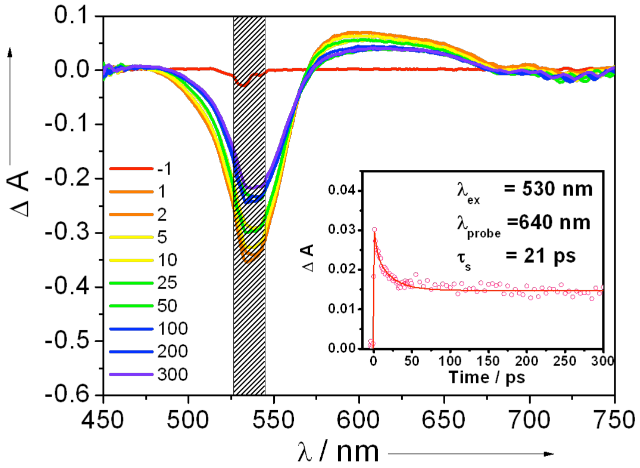

Fig. S13 Transient absorption spectra of **12**. The inset shows the decay profiles. λ_{ex} = 530 nm, λ_{probe} = 640 nm.

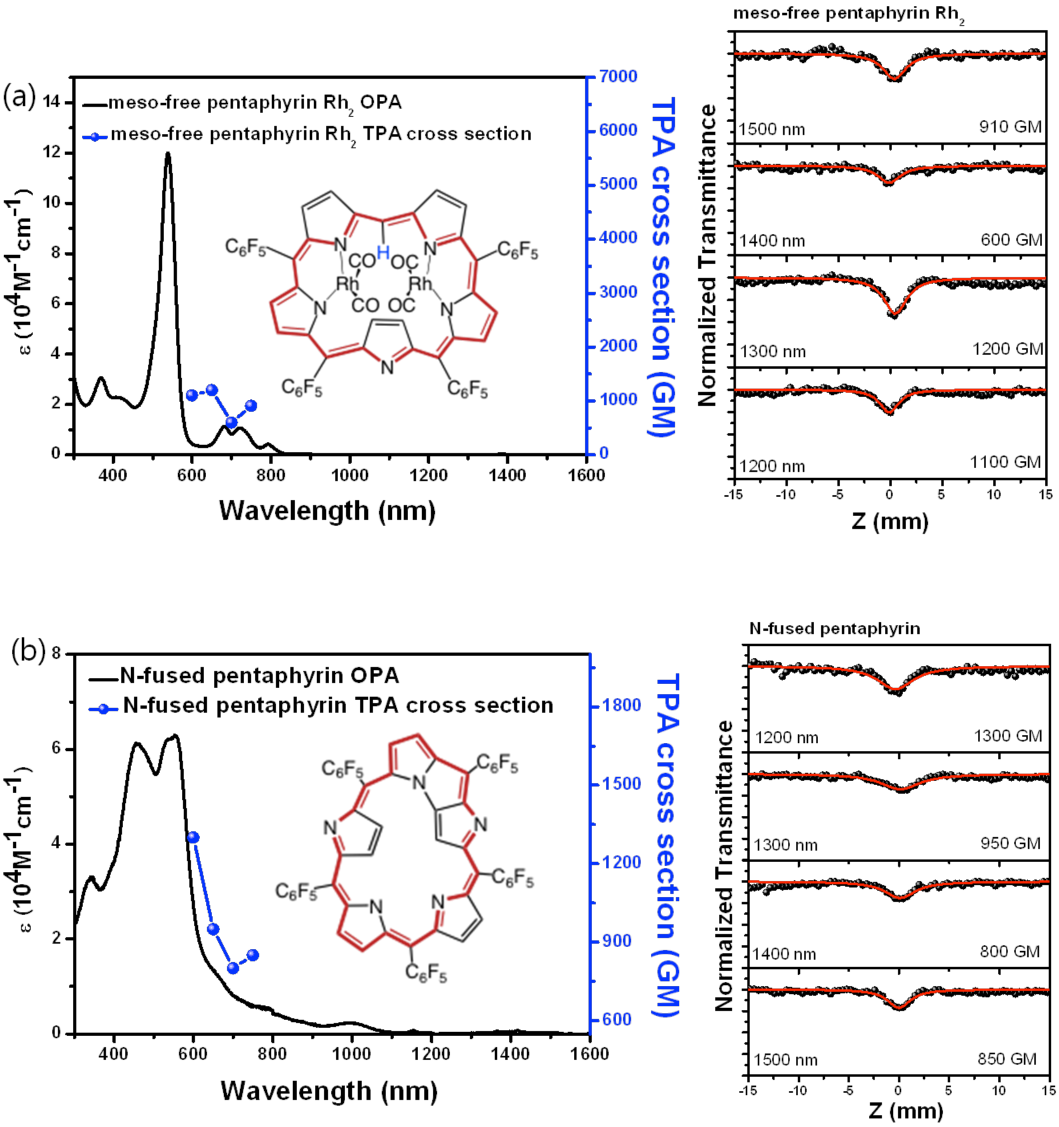

Fig. S14 One- (OPA) and two-photon absorption (TPA) spectra (left) and Z-scan curves (right) of (a) **12** and (b) **4** in CH_2Cl_2.

8. Full citation for reference 16

15. M. J. Frisch, G. W. Trucks, H. B. Schlegel, G. E. Scuseria, M. A. Robb, J. R. Cheeseman, G. Scalmani, V. Barone, B. Mennucci, G. A. Petersson, H. Nakatsuji, M. Caricato, X. Li, H. P. Hratchian, A. F. Izmaylov, J. Bloino, G. Zheng, J. L. Sonnenberg, M. Hada, M. Ehara, K. Toyota, R. Fukuda, J. Hasegawa, M. Ishida, T. Nakajima, Y. Honda, O. Kitao, H. Nakai, T. Vreven, J. A. Montgomery, Jr., J. E. Peralta, F. Ogliaro, M. Bearpark, J. J. Heyd, E. Brothers, K. N. Kudin,V. N. Staroverov, R. Kobayashi, J. Normand, K. Raghavachari,A. Rendell, J. C. Burant, S. S. Iyengar, J. Tomasi, M. Cossi, N. Rega, J. M. Millam, M. Klene, J. E. Knox, J. B. Cross, V. Bakken, C. Adamo, J. Jaramillo, R. Gomperts, R. E. Stratmann, O. Yazyev, A. J. Austin, R. Cammi, C. Pomelli, J. Ochterski, R. L. Martin, K. Morokuma, V. G. Zakrzewski, G. A. Voth, P. Salvador, J. J. Dannenberg, S. Dapprich, A. D. Daniels, O. Farkas, J. B. Foresman, J. V. Ortiz, J. Cioslowski, D. J. Fox, GAUSSIAN 09 *(Revision A.2)*, Gaussian, Inc., Wallingford, CT, 2009.